Molecular Plant Pathology

MOLECULAR PLANT PATHOLOGY (2017) 18(9), 1267–1281 DOI: 10.1111/mpp.12489

Resistance to citrus canker induced by a variant of *Xanthomonas citri* ssp. *citri* is associated with a hypersensitive cell death response involving autophagy-associated vacuolar processes

ROXANA A. ROESCHLIN[1], MARÍA A. FAVARO[1], MARÍA A. CHIESA[1], SERGIO ALEMANO[2], ADRIÁN A. VOJNOV[3], ATILIO P. CASTAGNARO[4], MARÍA P. FILIPPONE[4], FREDERICK G. GMITTER JR[5], JOSÉ GADEA[6,*] AND MARÍA R. MARANO[1,*]

[1]*Instituto de Biología Molecular y Celular de Rosario (IBR)–Consejo Nacional de Investigaciones Científicas y Tecnológicas (CONICET), Área Virología, Facultad de Ciencias Bioquímicas y Farmacéuticas, Universidad Nacional de Rosario (UNR), Ocampo y Esmeralda s/n, Rosario S2000FHN, Argentina*

[2]*Laboratorio de Fisiología Vegetal, Departamento de Ciencias Naturales, Facultad de Ciencias Exactas, Físico-Químicas y Naturales, Universidad Nacional de Río Cuarto, Ruta 36 Km. 601, Río Cuarto X5804ZAB, Córdoba, Argentina*

[3]*Instituto de Ciencia y Tecnología Dr. Cesar Milstein, Fundación Pablo Cassará-CONICET, Saladillo 2468, Ciudad de Buenos Aires C1440FFX, Argentina*

[4]*Instituto de Tecnología Agroindustrial del Noroeste Argentino (ITA-NOA), Estación Experimental Agroindustrial Obispo Colombres (EEAOC)-CONICET, Av. William Cross 3150, Las Talitas, Tucumán T4101XAC, Argentina*

[5]*Citrus Research and Education Center (CREC), University of Florida, 700 Experiment Station Rd., Lake Alfred, FL 33850, USA*

[6]*Instituto de Biología Molecular y Celular de Plantas (IBMCP), Universidad Politécnica de Valencia (UPV)-Consejo Superior de Investigaciones Científicas (CSIC), Ciudad Politécnica de la Innovación (CPI), Ed. 8E, C/Ingeniero Fausto Elio s/n, Valencia 46022, Spain*

SUMMARY

Xanthomonas citri ssp. *citri* (*X. citri*) is the causal agent of Asiatic citrus canker, a disease that seriously affects most commercially important *Citrus* species worldwide. We have identified previously a natural variant, *X. citri* A^T, that triggers a host-specific defence response in *Citrus limon*. However, the mechanisms involved in this canker disease resistance are unknown. In this work, the defence response induced by *X. citri* A^T was assessed by transcriptomic, physiological and ultrastructural analyses, and the effects on bacterial biofilm formation were monitored in parallel. We show that *X. citri* A^T triggers a hypersensitive response associated with the interference of biofilm development and arrest of bacterial growth in *C. limon*. This plant response involves an extensive transcriptional reprogramming, setting in motion cell wall reinforcement, the oxidative burst and the accumulation of salicylic acid (SA) and phenolic compounds. Ultrastructural analyses revealed subcellular changes involving the activation of autophagy-associated vacuolar processes. Our findings show the activation of SA-dependent defence in response to *X. citri* A^T and suggest a coordinated regulation between the SA and flavonoid pathways, which is associated with autophagy mechanisms that control pathogen invasion in *C. limon*. Furthermore, this defence response protects *C. limon* plants from disease on subsequent challenges by pathogenic *X. citri*. This knowledge will allow the rational exploitation of the plant immune system as a biotechnological approach for the management of the disease.

**Correspondence*: Email: marano@ibr-conicet.gov.ar; jgadeav@ibmcp.upv.es

Keywords: autophagy, biofilm formation, biological control, citrus canker resistance, hypersensitive response, salicylic acid, secondary metabolites.

INTRODUCTION

Xanthomonas citri ssp. *citri* (*X. citri*) strain A is the causative agent of Asiatic citrus canker, a disease that seriously affects most commercially important *Citrus* spp. worldwide (Vojnov *et al.*, 2010). In South America, other phylogenetically different canker-causing *Xanthomonas* have been identified, belonging to *X. fuscans* ssp. *aurantifolii* (*X. aurantifolii*) strains B and C (Schaad *et al.*, 2005, 2006). However, *X. aurantifolii* B strain could not be isolated from the field after Asiatic citrus canker became endemic in 2002 (Chiesa *et al.*, 2013), and *X. aurantifolii* C strain has a host range restricted to Mexican lime (*Citrus aurantifolia*) in some citrus-producing areas in Brazil (Graham *et al.*, 2004). Therefore, B and C strains are not a serious threat in the field.

Xanthomonas citri ssp. *citri* is a hemibiotrophic pathogen that grows and persists as epiphytes, forming biofilms on the host surface prior to endophytic colonization of the intercellular spaces of the mesophyll tissue through natural openings, such as stomata, or through wounds (Rigano *et al.*, 2007). A balance between biofilm formation and bacterial dispersion is essential to enhance the epiphytic persistence of bacteria prior to colonization and to circumvent the plant defence response (Favaro *et al.*, 2014; Vojnov and Marano, 2015).

The host defence response is composed of complex and highly regulated molecular networks, which can be triggered by the perception of either conserved pathogen-associated molecular

patterns (PAMPs) or race-specific pathogen effectors (Jones and Dangl, 2006; Macho and Zipfel, 2015). In *Citrus* spp., the first level of defence triggered by *X. citri* has been associated with early molecular changes in gene expression, particularly linked to the production of reactive oxygen species (ROS) (Cernadas *et al.*, 2008; Enrique *et al.*, 2011). However, in most cases, *X. citri* disrupts PAMP-triggered immunity (PTI) and produces the disease. In the last decade, different molecular and genetic approaches, including comparative genomics and mutants, have been followed to identify *X. citri* virulence factors or effectors involved in the suppression of PTI, leading to canker development. Recently, we have shown that xanthan, the major exopolysaccharide secreted by *Xanthomonas* spp., promotes *C. limon* susceptibility to *X. citri* by suppressing hydrogen peroxide (H_2O_2) accumulation (Enrique *et al.*, 2011). The *pthA4* gene encoding type III-secreted transcriptional activator-like (TAL) effector is another well-known pathogenicity effector of canker-causing *Xanthomonas* that contributes to host susceptibility (Duan *et al.*, 1999; Shiotani *et al.*, 2007). Deletion of the *pthA4* gene has been shown to reduce the bacterial population and abolish the ability of the pathogen to cause canker disease (Duan *et al.*, 1999; Soprano *et al.*, 2013).

The second level of plant immunity is triggered in many plant–pathogen interactions when specific effectors secreted by the pathogen can be recognized by plant resistance (R) proteins, activating effector-triggered immunity (ETI) (Jones and Dangl, 2006). However, no *R* gene has been identified in citrus to date. Several types of citrus and closely related genera, including 'Chinese' citron (*C. medica*), calamondin (*C. mitis* Blanco), Yuzu (*C. ichangensis* × *C. reticulata* var. *austera*) and 'Nagami' kumquat (*Fortunella margarita*), have been reported to be fully resistant to *X. citri*, suggesting a specific recognition of avirulence effectors (Chen *et al.*, 2012; Deng *et al.*, 2010; Khalaf *et al.*, 2011; Lee *et al.*, 2009). In this regard, transcriptional responses to *X. citri* in 'Nagami' kumquat include the induction of defence-related genes, particularly those implicated in the hypersensitive response (HR) associated with rapid programmed cell death (PCD), a process that restricts the spread of the pathogen and prevents disease development (Khalaf *et al.*, 2011). In Arabidopsis, HR-PCD induced by avirulent (hemi)biotrophic pathogens is associated with the activation of autophagy, an intracellular membrane trafficking pathway with substantial roles in both promotion and control of vacuole-mediated cell death (Teh and Hofius, 2014). The formation of autophagy vesicles is mediated by autophagy-related (ATG) proteins. In particular, the conversion from free ATG8 to ATG8-phosphatidylethanolamine (ATG8-PE) adducts has been reported to be a biochemical marker for the monitoring of autophagy processes (Hofius *et al.*, 2009; Teh and Hofius, 2014). Nevertheless, in canker-resistant genotypes, the mechanisms underlying HR-PCD remain obscure.

Xanthomonas citri ssp. *citri* natural variants with restricted host range have been isolated worldwide. Two of these variants, named A* and A^w, have a host range restricted to *C. aurantifolia* and *C. macrophylla* and induce HR-like reactions in *C. paradisi* and *C. sinensis* (Sun *et al.*, 2004; Vernière *et al.*, 1998). This HR-like phenotype is correlated with the presence of the *xopAG* (syn. *avrGf1*) effector gene, identified in all A^w strains and in three A* strains (Escalon *et al.*, 2013; Rybak *et al.*, 2009). However, the signalling pathways involved in these HR-like responses remain to be elucidated.

Recently, we have characterized a new variant of *X. citri*, named A^T, which shares more than 90% genetic similarity with the type A pathogenic strain *X. citri* T. Despite this high similarity, the host range of this variant is restricted to *C. aurantifolia* and *C. clementina*. In *C. limon*, this strain triggers an atypical chlorotic phenotype associated with a host-specific defence response (Chiesa *et al.*, 2013).

In this work, we assess the molecular and cellular events underlying the response of *C. limon* to *X. citri* A^T. We show that this variant triggers an HR-PCD associated with the interference of biofilm development and the activation of autophagy-related vacuolar processes. The defence response involves cell wall reinforcement, the accumulation of phenolic compounds and the induction of the salicylic acid (SA) signalling pathway. Moreover, pre-inoculation with *X. citri* A^T confers resistance to the pathogenic strain *X. citri* T.

RESULTS

Biofilm formation is impaired and bacterial growth is arrested in the *C. limon–X. citri* A^T interaction

Proper biofilm formation is a requirement for the achievement of maximal *X. citri* virulence (Malamud *et al.*, 2013), and the ability of canker-resistant *Citrus* spp. to interfere with this process has been reported in 'Okitsu' mandarin (Favaro *et al.*, 2014). In this work, we examined whether the impaired ability of *X. citri* A^T to cause disease in *C. limon* was associated with its inability to develop biofilms. Interestingly, no significant differences were observed between *X. citri* A^T and the pathogenic *X. citri* T strain in either initial adhesion (1–3 h) or biofilm development (15–24 h) to polystyrene microplates (Fig. S1, see Supporting Information). Next, green fluorescent protein (GFP)-tagged *X. citri* strains were inoculated in young *C. limon* leaves and the ability of *X. citri* A^T to develop biofilms and bacterial growth was monitored. Up to 2 days post-inoculation (dpi), epiphytic growth of both *X. citri* strains was similar on *C. limon* leaves (data not shown). At 7 dpi, biofilm formation was seen only with *X. citri* T and not with *X. citri* A^T (Fig. 1a). By contrast, both strains developed biofilms on *C. clementina* leaves (Fig. 1a). Here, both bacterial aggregates showed a three-dimensional structure on ZX-axis-projected images with the formation of compact microcolonies (Fig. 1a). These are similar structures to those reported previously for *X. citri*

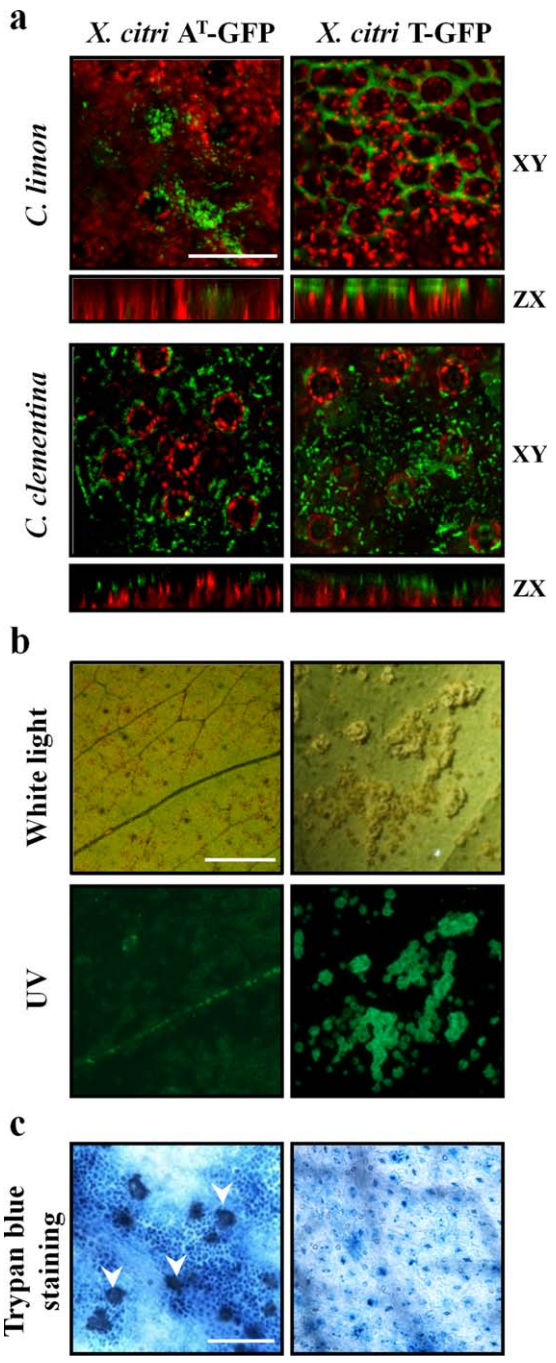

Fig. 1 Host-specific response triggered by *Xanthomonas citri* ssp. *citri* (*X. citri*) strain A^T. (a) Biofilm formation on *Citrus limon* and *C. clementina* leaves at 7 days post-inoculation (dpi). Red chlorophyll fluorescence and green signals from green fluorescent protein (GFP)-tagged *X. citri* strains are shown. XY and ZX are the XY- and ZX-axis-projected images, respectively. Scale bar, 50 μm. (b) Macroscopic symptoms in *C. limon* leaves at 20 dpi. Leaves were photographed under white and UV light. Scale bar, 10 mm. (c) Microscopic cell death phenotype (arrows) observed at 48 h post-inoculation. Scale bar, 150 μm.

biofilms formed on the susceptible genotypes *C. limon* and *C. clementina* (Favaro *et al.*, 2014; Rigano *et al.*, 2007). Moreover, inoculation of both strains onto *C. clementina* leaves led to the development of cankerous lesions at 20 dpi (data not shown). Nevertheless, *X. citri* A^T and T elicited different macroscopic symptoms in *C. limon* leaves at 20 dpi; *X. citri* A^T induced discrete black spots, phenotypically different from the canker lesions caused by *X. citri* T (Fig. 1b). Trypan blue staining revealed that *X. citri* A^T induced the cell death response at 48 hpi in *C. limon*, whereas no cell death was observed after inoculation of *X. citri* T over the monitored period (Fig. 1c).

Taken together, these results indicate that *X. citri* A^T is able to form microcolonies and develop biofilms on both non-biotic and certain biotic surfaces, and suggest that it is the induction of defence responses specifically in *C. limon* that interferes with biofilm development and the arrest of bacterial growth.

A distinct set of *C. limon* genes mediates canker resistance

Transcriptome analysis was performed to gain insight into the molecular mechanisms mediating the cell death phenotype observed in *C. limon* plants inoculated with *X. citri* A^T. Leaves were inoculated with bacterial suspensions of both *X. citri* strains and samples were harvested at 48 h post-inoculation (hpi). Differential gene expression analysis identified 1079 up-regulated and 1832 down-regulated genes in the interaction with *X. citri* A^T [fold change ≥ 2 in inoculated vs. non-treated plants; false discovery rate (FDR) $\leq 5\%$]. A lower but substantial number of genes were differentially expressed in the compatible *C. limon*–*X. citri* T interaction (869 and 1036 up- and down-regulated, respectively) (Table S2, see Supporting Information). Comparison of both transcriptomic responses revealed that an important number of genes were specifically expressed only by one of the two bacteria (Fig. S2, see Supporting Information). In particular, 1455 genes (461 and 994 up- and down-regulated, respectively) were unique to the *X. citri* A^T response (Table S3, see Supporting Information). Functional analysis identified 104 gene ontology (GO) categories statistically enriched in the *X. citri* A^T interaction and 62 in the *X. citri* T interaction. Again, as observed at the transcript level, we found a number of biological processes that were distinct between the two interactions (Tables S4 and S5, see Supporting Information). The most significant 30 categories according to REVIGO (Supek *et al.*, 2011) are shown in Table 1.

These data indicate that both strains trigger an important rearrangement of the *C. limon* transcriptome and, although some of these responses are shared by the two interactions, there are distinct responses that are exclusively triggered by *X. citri* A^T. Some of these processes were studied in detail using a combination of molecular, physiological and ultrastructural analyses.

Table 1 Representative subset of the gene ontology (GO) 'biological process' terms of *Citrus limon–Xanthomonas citri* ssp. *citri* (*X. citri*) strains.

	GO term	Description	Adjusted *P* value
X. citri A^T			
Up-regulated	GO:0006790	Sulfur compound metabolic process	8.69E-05
	GO:0009813	Flavonoid biosynthetic process	3.62E-04
	GO:0009636	Response to toxic substance	3.80E-04
	GO:0045454	Cell redox homeostasis	7.01E-04
	GO:0009072	Aromatic amino acid family metabolic process	1.61E-03
	GO:0008299	Isoprenoid biosynthetic process	2.47E-03
	GO:0009751	Response to salicylic acid	2.47E-03
	GO:0015031	Protein transport	5.80E-03
	GO:0006081	Cellular aldehyde metabolic process	1.07E-02
	GO:0006820	Anion transport	1.24E-02
	GO:0009073	Aromatic amino acid family biosynthetic process	1.45E-02
	GO:0009814	Defence response, incompatible interaction	1.47E-02
	GO:0019760	Glucosinolate metabolic process	1.60E-02
	GO:0009407	Toxin catabolic process	1.83E-02
	GO:0009873	Ethylene-activated signalling pathway	2.53E-02
	GO:0015833	Peptide transport	2.74E-02
	GO:0052543	Callose deposition in cell wall	2.88E-02
	GO:0015694	Mercury ion transport	2.88E-02
	GO:0046246	Terpene biosynthetic process	2.88E-02
	GO:0006801	Superoxide metabolic process	3.41E-02
	GO:0052386	Cell wall thickening	3.41E-02
	GO:0009627	Systemic acquired resistance	3.55E-02
	GO:0009915	Phloem sucrose loading	3.75E-02
	GO:0043090	Amino acid import	3.75E-02
	GO:0016042	Lipid catabolic process	4.05E-02
	GO:0016070	RNA metabolic process	4.35E-02
	GO:0043043	Peptide biosynthetic process	4.93E-02
	GO:0009805	Coumarin biosynthetic process	4.94E-02
Down-regulated	GO:0010154	Fruit development	1.45E-08
	GO:0009755	Hormone-mediated signalling pathway	1.71E-06
	GO:0009639	Response to red or far-red light	1.52E-05
	GO:0008544	Epidermis development	1.35E-04
	GO:0015979	Photosynthesis	1.96E-04
	GO:0007018	Microtubule-based movement	3.11E-04
	GO:0042493	Response to drug	3.11E-04
	GO:0050790	Regulation of catalytic activity	3.23E-04
	GO:0030163	Protein catabolic process	5.54E-04
	GO:0048589	Developmental growth	1.04E-03
	GO:0006163	Purine nucleotide metabolic process	1.09E-03
	GO:0048229	Gametophyte development	1.25E-03
	GO:0000902	Cell morphogenesis	1.90E-03
	GO:0009808	Lignin metabolic process	2.62E-03
	GO:0010015	Root morphogenesis	2.74E-03
	GO:0007010	Cytoskeleton organization	3.24E-03
	GO:0009555	Pollen development	3.80E-03
	GO:0006855	Drug transmembrane transport	4.39E-03
	GO:0006096	Glycolytic process	5.32E-03
	GO:0006508	Proteolysis	5.38E-03
	GO:0016568	Chromatin modification	6.99E-03
	GO:0006260	DNA replication	7.99E-03
	GO:0032268	Regulation of cellular protein metabolic process	7.99E-03
	GO:0006164	Purine nucleotide biosynthetic process	8.63E-03
	GO:0048827	Phyllome development	1.27E-02
	GO:0006006	Glucose metabolic process	1.37E-02
	GO:0010118	Stomatal movement	1.72E-02
	GO:0010158	Abaxial cell fate specification	1.86E-02
	GO:0010588	Cotyledon vascular tissue pattern formation	2.47E-02

Table 1 *Continued*

	GO term	Description	Adjusted *P* value
	GO:0010205	Photoinhibition	2.47E-02
X. citri T			
Up-regulated	GO:0009408	Response to heat	2.13E-11
	GO:0007047	Cell wall organization	9.58E-05
	GO:0042744	Hydrogen peroxide catabolic process	1.81E-04
	GO:0009698	Phenylpropanoid metabolic process	1.37E-03
	GO:0006949	Syncytium formation	8.58E-03
	GO:0016052	Carbohydrate catabolic process	9.09E-03
	GO:0009827	Plant-type cell wall modification	1.40E-02
	GO:0006412	Translation	1.50E-02
	GO:0042547	Cell wall modification involved in multidimensional cell growth	2.84E-02
	GO:0032508	DNA duplex unwinding	2.84E-02
	GO:0009620	Response to fungus	3.17E-02
	GO:0009807	Lignan biosynthetic process	4.48E-02
Down-regulated	GO:0006811	Ion transport	1.22E-10
	GO:0006812	Cation transport	5.09E-09
	GO:0030003	Cellular cation homeostasis	3.09E-08
	GO:0006351	Transcription, DNA dependent	2.27E-06
	GO:0007166	Cell surface receptor signalling pathway	2.94E-06
	GO:0016070	RNA metabolic process	5.15E-06
	GO:0006721	Terpenoid metabolic process	4.77E-04
	GO:0006814	Sodium ion transport	6.66E-04
	GO:0009723	Response to ethylene stimulus	8.29E-04
	GO:0010386	Lateral root formation	1.33E-03
	GO:0010104	Regulation of ethylene-mediated signalling pathway	1.86E-03
	GO:0051607	Defence response to virus	4.16E-03
	GO:0008610	Lipid biosynthetic process	6.65E-03
	GO:0006281	DNA repair	8.06E-03
	GO:0010380	Regulation of chlorophyll biosynthetic process	1.19E-02
	GO:0010017	Red or far-red light signalling pathway	1.20E-02
	GO:0006021	Inositol biosynthetic process	1.51E-02
	GO:0009308	Amine metabolic process	1.67E-02
	GO:0009944	Polarity specification of adaxial/abaxial axis	2.24E-02
	GO:0005992	Trehalose biosynthetic process	2.69E-02
	GO:0019752	Carboxylic acid metabolic process	2.99E-02
	GO:0009690	Cytokinin metabolic process	3.14E-02
	GO:0010586	miRNA metabolic process	3.19E-02
	GO:0009968	Negative regulation of signal transduction	3.37E-02
	GO:0045017	Glycerolipid biosynthetic process	3.37E-02
	GO:0009735	Response to cytokinin stimulus	4.16E-02
	GO:0048573	Photoperiodism, flowering	4.45E-02
	GO:0051762	Sesquiterpene biosynthetic process	4.72E-02

First 30 significant GO terms summarized by REVIGO (Supek *et al.*, 2011) are shown (adjusted *P* value ≤ 0.05). 'Up-regulated': GO terms enriched in the up-regulated genes. 'Down-regulated': GO terms enriched in the down-regulated genes.

Defence response to *X. citri* A^T is associated with cell wall reinforcement and the accumulation of phenolic compounds

Different genes related to cell wall modification were regulated in response to both *X. citri* strains, probably influencing the final outcome of each interaction. In *C. limon*, *X. citri* A^T down-regulates genes such as xyloglucan:xyloglucosyl transferases *XTH6* and *XTH16* (repressed by 2.8-fold), involved in cell wall loosening, cellulose synthases *CESA7* and *CSLC12* (repressed by 3.8- and three-fold, respectively), pectinesterases, such as *PME3* and *SKS6* (repressed by 4.1 and 3.8-fold, respectively), and β-1,3-glucanases (repressed by 3.3-fold), suggesting an active reinforcement of the plant cell wall through the increase in pectin methyl esterification and callose deposition (Table S3). Conversely, *X. citri* T up-regulates expansin genes, such as *βEXP2* and *EXPA4* (induced by 64- and 2.7-fold, respectively), which promote the weakening of the plant cell wall, resulting in cell enlargement (hypertrophy) and division (hyperplasia) required for canker development (Cernadas *et al.*, 2008; Fu *et al.*, 2012) (Table S3). *βEXP2* expression was also analysed by quantitative reverse

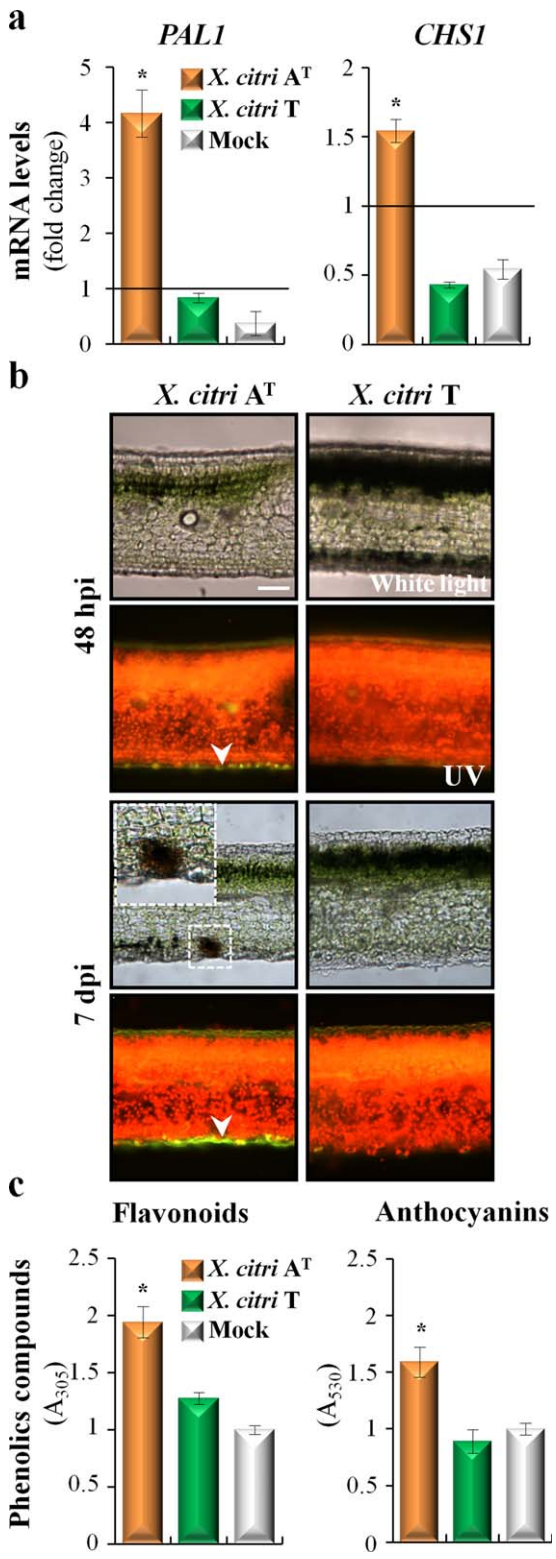

Fig. 2 Phenolic compounds are involved in the *Citrus limon* response to *Xanthomonas citri* ssp. *citri* (*X. citri*) strain A^T. (a) Quantitative reverse transcription-polymerase chain reaction analysis of phenylalanine ammonia lyase (*PAL1*) and chalcone synthase (*CHS1*) mRNAs measured at 48 h post-inoculation (hpi). The relative gene expression ($\Delta\Delta Ct$) fold change of mRNA levels was performed considering non-treated plants as reference samples and a histone H4 transcript as an endogenous control. Values are expressed as means ± standard deviation (SD) from three independent biological replicates. The dataset marked with an asterisk is significantly different as assessed by Tukey's test ($P < 0.05$). (b) Light microscopic images of lemon leaves inoculated with *X. citri* strains. Leaves were photographed at 48 hpi and 7 days post-inoculation (dpi) under white and UV light. Green fluorescent polyphenolic compounds (arrows) and red chlorophyll fluorescence are observed. The presence of discrete black spots in the *C. limon*–*X. citri* A^T interaction is shown enlarged in the top inset. Scale bar, 10 μm. (c) Spectrophotometric determination of flavonoids and anthocyanins at 48 hpi. Values are expressed as means ± SD. Each sample consists of 10 leaf discs (0.5 cm in diameter) obtained from two shoots of three different plants, and 10 biological replicates were performed. The dataset marked with an asterisk is significantly different as assessed by Tukey's test ($P < 0.05$). A, absorbance.

transcription-polymerase chain reaction (qRT-PCR), confirming the microarray results (Table S6, see Supporting Information). Functional analysis using GO also revealed that categories such as 'cell wall thickening' (adjusted *P* value, 3.4×10^{-2}) and 'defence response by callose deposition in cell wall' (adjusted *P* value, 2.5×10^{-2}) were enriched in up-regulated genes by *X. citri* A^T (Table 1). However, the category 'cell wall modification involved in multidimensional cell growth' (adjusted *P* value, 2.8×10^{-2}) was enriched in the *C. limon*–*X. citri* T interaction (Table 1). Taken together, these results suggest that the *C. limon* response to *X. citri* A^T is associated with fortification of the cell wall, limiting the growth and spread of the bacteria.

The category 'flavonoid biosynthetic process' (adjusted *P* value, 3.6×10^{-4}) was enriched in genes up-regulated by *X. citri* A^T, suggesting that the biosynthesis of this secondary metabolite is fostered in this interaction (Table 1). In particular, genes such as phenylalanine ammonia lyase (*PAL1*) (induced by 2.9-fold), chalcone synthase (*CHS1*) (induced by four-fold), flavanone 3-hydroxylase (*F3H*) (induced by two-fold), flavonol 3′-hydroxylase (F3′H) (induced by three-fold), downy mildew resistant 6 (*DMR6*) (induced by 5.5-fold) and anthocyanidin-3-O-glucosyltransferase (*3GT*) (induced by 2.3-fold) were all up-regulated only in response to *X. citri* A^T (Table S3). The same trend was observed by qRT-PCR for *PAL1* and *CHS1*, as observed in Fig. 2a. Confirming these results, histological assays showed the accumulation of bright green fluorescent polyphenolic compounds, particularly on the abaxial side and around stomata, in *X. citri* A^T-inoculated leaves at 48 hpi (Fig. 2b). Notably, this accumulation was higher at 7 dpi, particularly surrounding dead cells (Figs 2b and S3, see Supporting Information). By contrast, leaves inoculated with *X. citri* T did not show the accumulation of phenolic compounds, as indicated by the homogeneous red fluorescence along the tissue, generated by the autofluorescence of chlorophyll (Fig. 2b). Moreover, spectrophotometric determinations confirmed that the content of flavonoids and anthocyanins increased significantly in response to

X. citri A^T, supporting the idea that phenolic compounds are implicated in this host-specific defence response (Fig. 2c).

X. citri A^T down-regulates genes related to ROS scavenging and photosynthesis

The production of ROS is one of the earliest cellular responses following successful pathogen recognition. Apoplastic generation of superoxide (O_2^-) or its dismutation product H_2O_2 can cause strengthening of the plant cell walls, mediation of signalling for gene activation and promotion of HR-PCD (Chi *et al.*, 2013). It has been observed previously that the *C. limon*–*X. citri* A^T interaction leads to an increased production of H_2O_2 (Chiesa *et al.*, 2013), suggesting the deployment of a bona fide defence response leading to canker resistance. Several ROS-related genes regulated in response to *X. citri* A^T inoculation were found in this work, indicating that redox homeostasis is altered in the plant cell (Table S2). Microarray data indicated that a respiratory burst NADPH-oxidase homologue to Arabidopsis *RBOHD*, the main enzyme responsible for the oxidative burst on pathogen infection (Kadota *et al.*, 2014), was induced 5.2-fold, a result that was confirmed by qRT-PCR (Tables S2 and S6). In addition, copper/zinc superoxide dismutase (*SOD2*) and its chaperone (*CCS*) increased their expression 2.3-fold, whereas ROS scavengers, such as catalases (*CAT3*) or peroxidases (*PER64*, *PER68*), were down-regulated (Table S3). A different redox response was observed in leaves inoculated with the pathogenic *X. citri* T. Although the expression of the *RBOHD* gene was also slightly up-regulated, this induction was two-fold lower than in the *X. citri* A^T interaction (Table S2). Moreover, the 'hydrogen peroxide catabolic process' was enriched (adjusted *P* value, 1.8×10^{-4}) (Table 1).

In addition, the GO category related to 'photosynthesis' was enriched in the down-regulated genes in response to *X. citri* A^T (adjusted *P* value, 1.9×10^{-4}; Table 1). This category includes genes encoding thylakoid proteins, such as the light-harvesting complex (*LHCB6* and *LCHB1.4*), components of the oxygen-evolving complex of photosystem II (*PSBO-1* and *PSBO-2*) and genes involved in the Calvin cycle (*RBCS1A*, *RBCS2B*, *FBA1* and *RCA*) (Table S3). This rapid down-regulation of photosynthesis may also be associated with the high level of ROS production shown in the *C. limon*–*X. citri* A^T interaction, as demonstrated in ETI responses (Liu *et al.*, 2007; Shapiguzov *et al.*, 2012).

SA is involved in the local defence response induced by *X. citri* A^T

SA is thought to act with ROS in a feed-forward loop, promoting HR-PCD, as demonstrated in defence responses against (hemi)biotrophic pathogen infections (Mammarella *et al.*, 2014; Wrzaczek *et al.*, 2013). Interestingly, functional analysis identified the GO category 'response to salicylic acid' enriched in the up-regulated genes unique to the *C. limon*–*X. citri* A^T interaction (adjusted *P* value, 2.4×10^{-3}; Table 1). Belonging to this category, genes involved in SA biosynthesis, signalling and response were up-regulated. For instance, as described previously, the expression of *PAL1* was induced 2.9-fold, and genes involved in the biosynthesis of methylsalicylate, such as *S*-adenosylmethionine-dependent methyltransferases (*SAMT* and *BSMT1)*, were induced 2.4 and 4.4-fold, respectively. The same tendency was found for the key regulator of SA signalling, nonexpressor of pathogenesis-related genes 1 (*NPR1*, 2.6-fold), the transcription factor *WRKY70* (4.4-fold) and the pathogenesis-related (*PR*) genes *PR1* (32.7-fold) and *PR4* (14.1-fold) (Table S3). The induction of the first three key genes of the SA pathway was confirmed by qRT-PCR (Fig. 3a).

SA quantification showed that its concentration increased three-fold in *X. citri* A^T-inoculated leaves at 48 hpi when compared with control samples (Fig. 3b). This increase was not observed at 7 dpi (Fig. 3b), which is also associated with the return to basal levels of *WRKY70* and *PR1* gene expression (data not shown). Interestingly, at this time point, biofilm development began to decline (Fig. 1a), suggesting a temporal regulation of SA signalling in the defence response against *X. citri* A^T. No increases in SA levels were observed in *X. citri* T-inoculated leaves (Fig. 3b).

Subcellular analysis suggests autophagy-mediated vacuolar cell death events in *X. citri* A^T-inoculated *C. limon* leaves

In this work, it was shown that *X. citri* A^T triggers a host-specific defence response associated with HR-PCD. To further characterize the subcellular changes induced by *X. citri* A^T, samples from bacteria-inoculated leaves were analysed by transmission electron microscopy (TEM). Immediately after inoculation of *C. limon* (0 hpi), tissues did not present any cellular change (Fig. 4a,g). At 48 hpi, *X. citri* T-inoculated samples showed the presence of bacteria colonizing the leaf surface (Fig. 4b) and invading the mesophyll cells (Fig. 4c). At 7 dpi, bacteria were present within the damaged mesophyll cells (Fig. 4d), and became more abundant in the intercellular space at 20 dpi (Fig. 4e), when canker symptoms were already visible (Fig. 4f). Moreover, consistent with the ability of *X. citri* T and A^T to develop canker on *C. clementina*, ultrastructural changes associated with host cell wall dissolution and cell disruption were observed (Fig. S4, see Supporting Information).

By contrast, although *X. citri* A^T-inoculated *C. limon* leaves showed dispersed bacteria on the leaf surface (Fig. 4h) and in the intercellular space (Fig. 4i), the epidermal pavement cells were empty and tightly cemented at 48 hpi, suggesting cellular collapse that is characteristic of HR vacuolar cell death (van Doorn *et al.*, 2011; Hatsugai *et al.*, 2009; Rojo *et al.*, 2004). Associated with these processes, higher magnification images showed bacteria with an irregular cell shape undergoing degenerative processes (Fig. 4i). Furthermore, mesophyll cells showed vacuole membrane invaginations, suggesting a loss of vacuole turgor (Fig. 4j), and a

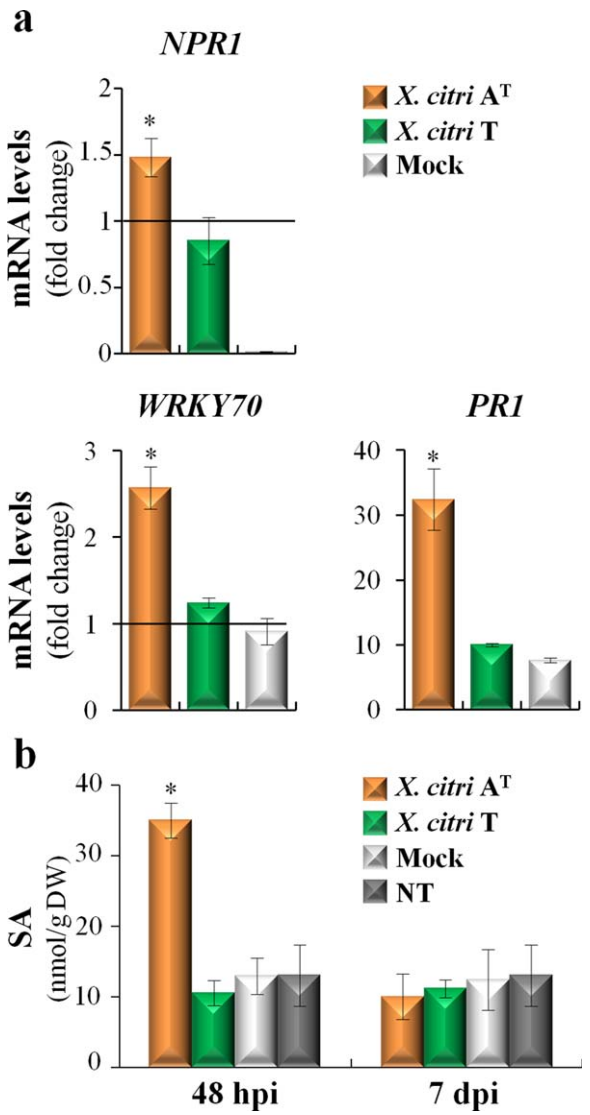

Fig. 3 *Xanthomonas citri* ssp. *citri* (*X. citri*) strain A^T triggers the accumulation of salicylic acid (SA) in *Citrus limon*. (a) Quantitative reverse transcription-polymerase chain reaction analysis of *NPR1* (nonexpressor of pathogenesis-related genes 1), *WRKY70* transcription factor and pathogenesis-related (*PR1*) mRNAs was measured at 48 h post-inoculation (hpi). The relative gene expression ($\Delta\Delta Ct$) fold change of mRNA levels was performed considering non-treated plants (NT) as reference samples and the histone H4 transcript as an endogenous control. Values are expressed as means ± standard deviation (SD) from three independent biological replicates. The dataset marked with an asterisk is significantly different as assessed by Tukey's test ($P < 0.05$). (b) Analysis of SA through liquid chromatography-tandem mass spectrometry (LC-MS/MS) performed at 48 hpi and 7 days post-inoculation (dpi). Values are expressed as means ± SD from three independent biological replicates. The dataset marked with an asterisk is significantly different as assessed by Tukey's test ($P < 0.05$). DW, dry weight.

perforated nuclear envelope wrapped by tubular extensions (Fig. 4k), all features of vacuolar cell death (van Doorn *et al.*, 2011).

Next, at 7 dpi, collapsed mesophyll cells were observed, suggesting the rupture of the tonoplast and the release of the vacuolar content (Fig. 4l). However, mesophyll cells with intact chloroplasts showed the presence of autophagosome-like vesicles (2.1 ± 0.05 autophagosomes per cell) (Fig. 4m). The formation of autophagosomes (double-membrane vesicles) is a hallmark of the activation of the authophagy-mediated pathway (van Doorn *et al.*, 2011). At 20 dpi, TEM analysis exhibited similar results to those obtained previously, showing two types of mesophyll cell response. Although some were dead, with thickening of the cell wall and the accumulation of electron-dense multitextured materials filling the intercellular space (Fig. 4n), others showed signs of chloroplast enlargement (Fig. 4o) and an increase in the number and size of autophagosomes (3.5 ± 0.12 autophagosomes per cell) (Fig. 4p,q), suggesting that an active autophagy-regulated mechanism could be involved in the restriction of the spread of HR-PCD. In addition, immunodetection of ATG8 proteins revealed a marked accumulation of free ATG8 isoforms and ATG8-PE adducts in *X. citri* A^T-inoculated *C. limon* leaves, and an increase in the conversion of ATG8 to ATG8-PE shows an active autophagic mechanism triggered by this bacterium (Fig. 5).

Taken together, these results suggest that *X. citri* A^T induces HR-PCD in *C. limon*, mediated by vacuolar cell death associated with autophagy. At early times post-inoculation, these autophagic processes would prevent bacterial colonization through vacuolar cell death, but, later, may restrict the spread of the cell death process itself.

X. citri A^T protects *C. limon* from canker development

In order to investigate whether the host response triggered by *X. citri* A^T is able to induce plant protection to the pathogenic strain *X. citri* T, young *C. limon* leaves were pre-inoculated by cotton swab with bacterial suspensions of *X. citri* A^T-GFP. At 48 hpi, the leaves were challenged with *X. citri* T-GFP by spraying (Fig. 6a). A significant reduction in canker development was observed in leaves pre-inoculated with *X. citri* A^T-GFP when compared with mock-inoculated leaves (Fig. 6b). Similar results were obtained when pre-inoculation with *X. citri* A^T-GFP was performed by spraying (data not shown). In a new assay, both bacteria were co-inoculated onto *C. limon* in equal amounts. Under these conditions, cankerous lesions were observed (Fig. 6c), indicating that bacterial competition is not the determinant of the *X. citri* A^T-induced protection observed previously.

These data suggest that *X. citri* A^T triggers a defence response that protects *C. limon* from canker disease.

DISCUSSION

X. citri A^T triggers a recognition event interfering with biofilm development in *C. limon*

In this work, we demonstrate that *X. citri* A^T is able to develop biofilms on *C. clementina* and to cause disease. The presence of *X. citri* A^T inside the damaged *C. clementina* mesophyll cells

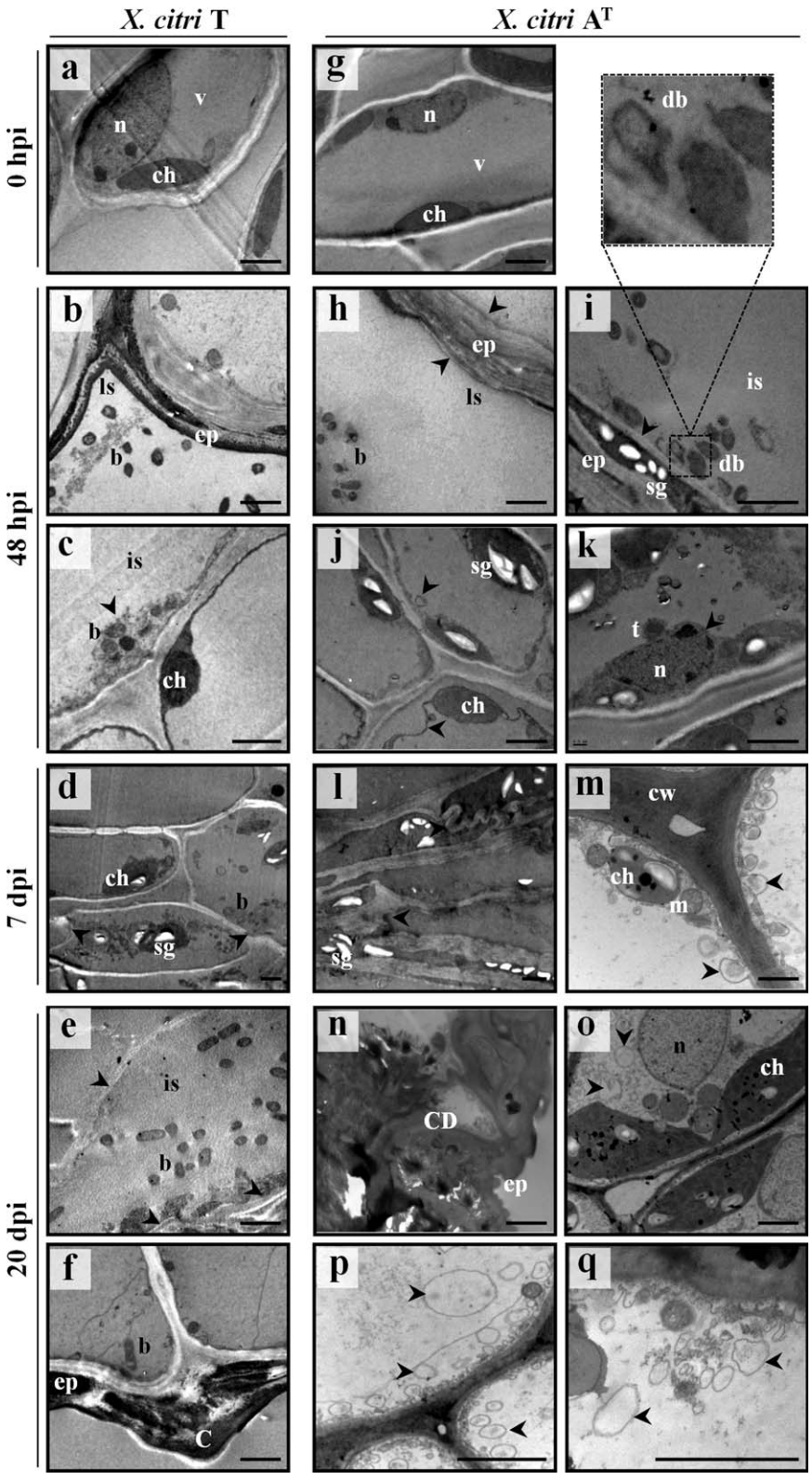

Fig. 4 Ultrastructural features of *Citrus limon* leaves inoculated with *Xanthomonas citri* ssp. *citri* (*X. citri*) strains. (a, g) At 0 h post-inoculation (hpi), the nucleus, vacuole and chloroplast are intact. (b) Bacteria are localized on the leaf surface and (c) within the mesophyll cells. (d) Bacteria colonizing mesophyll tissue. (e) Bacteria in the intercellular space. Arrows, electron-dense multitextured materials. (f) Breakdown of epidermal tissue and canker formation. (h) Bacteria colonizing the leaf surface and (i) the intercellular spaces. Arrows, epidermal tissue collapse. Top panel shows the magnification of degenerated bacteria. (j) Arrows, vacuole membrane invaginations. (k) Arrow, perforations of nuclear envelope. (l) Arrows, cellular collapse. (m) Arrows, autophagosome-like vesicles. (n) Cell death and accumulation of electron-dense multitextured materials. (o–q) Arrows, autophagosome-like vesicles. Scale bar, 2 μm. b, bacteria; C, canker; CD, cell death; ch, chloroplast; cw, cell wall; db, degenerated bacteria; ep, epidermis; is, intercellular space; ls, leaf surface; m, mitochondria; n, nucleus; sg, starch granules; t, tubular extensions; v, vacuole.

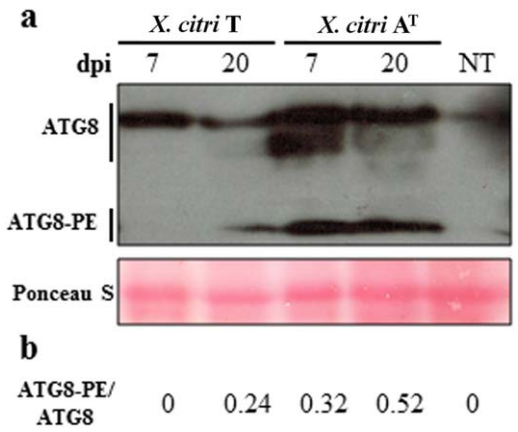

Fig. 5 Immunoblot assay to detect free ATG8 and ATG8-phosphatidylethanolamine (PE) adduct in *Citrus limon* inoculated with *Xanthomonas citri* ssp. *citri* (*X. citri*) strains. (a) Total protein was extracted from the inoculated tissues at 7 and 20 days post-inoculation (dpi) and subjected to sodium dodecylsulfate-polyacrylamide gel electrophoresis (SDS-PAGE) in the presence of urea, followed by immunoblot analyses with ATG8 antibody. The full lines locate the groups of free ATG8 isoforms and ATG8-PE adducts. Protein profiles in the lower panels were detected by Ponceau S staining of a polyvinylidene difluoride (PVDF) membrane. The experiment was repeated twice using three independent biological replicates, and a representative image is shown. (b) The ATG8-PE/ATG8 ratios were determined by the inmunodetection experiment shown in (a). NT, non-treated leaves.

implies the ability of these bacteria to dissolve the host cell wall and disrupt the cell, inducing similar morphological changes as pathogenic *X. citri* T. These ultrastructural modifications during citrus canker development have been well reported in *X. citri*-inoculated Mexican lime samples (Lee *et al.*, 2009). However, although *X. citri* A^T is able to colonize the leaf surface and the intercellular spaces of the mesophyll tissue, it fails to develop a mature biofilm structure in *C. limon*. The presence of degenerated *X. citri* A^T bacteria near the cell wall might be linked to the release of vacuolar hydrolytic enzymes during the HR-PCD response, affecting biofilm development. Altogether, these results indicate that bacterial biofilm formation constitutes not only a virulence factor of canker-causing *Xanthomonas*, but its disruption could also be used as a marker of the canker resistance response.

X. citri A^T triggers an HR-PCD response which is associated with elevated levels of flavonoids and SA

The phenotypes triggered by *X. citri* strains in *C. limon* are associated with extensive transcriptional reprogramming. An important degree of commonality between the two interactions with different outcome is found, which may be related to the similar genetic backgrounds of the two strains (Chiesa *et al.*, 2013). Therefore, this common subset of genes could account for the PTI basal response, as reported previously between *C. sinensis–X. aurantifolii* C and *C. sinensis–X. citri* interactions (Cernadas *et al.*, 2008).

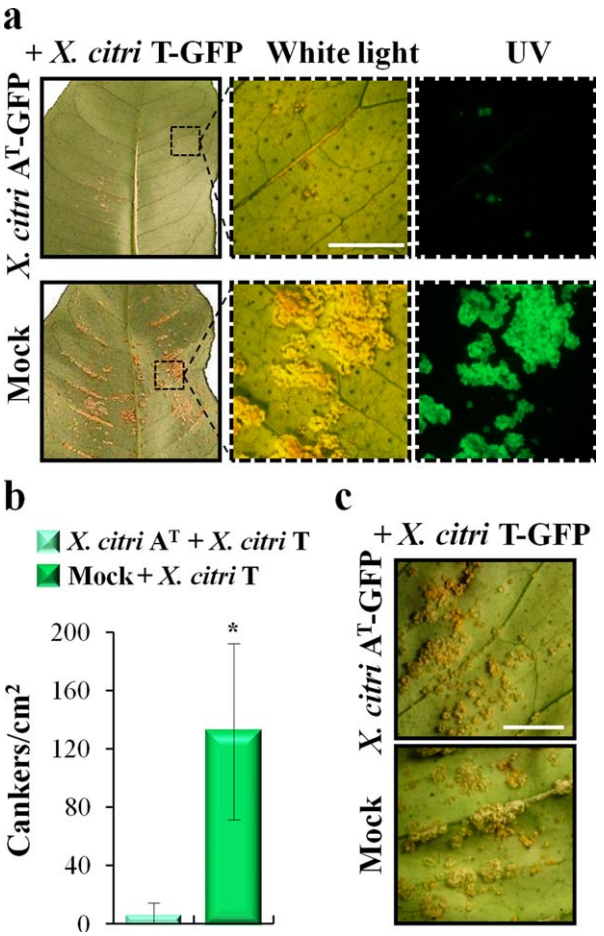

Fig. 6 Pre-inoculation with *Xanthomonas citri* ssp. *citri* (*X. citri*) strain A^T protects *Citrus limon* from canker disease. (a) Phenotypic response of lemon leaves pre-inoculated with *X. citri* A^T tagged with green fluorescent protein (GFP) or mock-inoculated by cotton swab. At 48 h post-inoculation, the leaves were subsequently challenged, via spraying, with the pathogenic *X. citri* T-GFP strain. Sections from the left panels are shown magnified in the right panels. Leaves were photographed under white and UV light. Scale bar, 10 mm. (b) Number of canker lesions per square centimetre in pre-inoculated leaves at 20 days post-inoculation (dpi). Values are expressed as means ± standard deviation (SD) from three independent biological replicates, each involving three different plants and five different leaves per plant. The dataset marked with an asterisk is significantly different as assessed by Student's *t*-test ($P < 0.05$). (c) Canker symptoms, developed at 20 dpi, of lemon leaves co-inoculated with equal amounts of both bacterial strains by cotton swab. Scale bar, 10 mm.

The most striking differences are observed in the number of unique genes regulated during *X. citri* A^T infection when compared with the response to pathogenic *X. citri* T. From the total of the unique genes considered to be differentially expressed, nearly 76% correspond to the *X. citri* A^T-triggered response. In a similar way, *X. aurantifolii* C induces a greater number of defence-related genes than *X. citri* infection in *C. sinensis*, suggesting that the

amplitude of this response is sufficient to halt *X. aurantifolii* C growth and to establish an effective HR (Cernadas *et al.*, 2008). In contrast, a relatively small number of defence-related genes were up-regulated in the partially resistant 'Meiwa' kumquat cultivar to *X. citri*, when compared with susceptible *C. sinensis* (Fu *et al.*, 2012). Overall, our results are consistent with the contention that the *C. limon* defence response to *X. citri* A^T is governed by the recognition of bacterial effectors. Another remarkable feature of the resistance response is that the number of repressed genes is doubled when compared with the susceptible response (pathogenic interaction). The down-regulation of genes coding for development and photosynthesis proteins, coupled with the up-regulation of genes coding for defence proteins, points to a possible cross-talk between these biological processes in the infected tissue. This regulation would allow a better management of the energy resources, as reported previously in other interactions that are known to be mediated by ETI (Bilgin *et al.*, 2010; Karpinski *et al.*, 2013).

The maintenance of host cell wall integrity in response to *X. citri* A^T, through the repression of the xyloglucan-cellulose network and the production of highly methyl-esterified pectins, may protect it from bacterial enzymatic degradation. The fact that the increase in PME activity leads to enhanced *Pseudomonas syringae* susceptibility in Arabidopsis reinforces this idea (Bethke *et al.*, 2014). Interestingly, *X. aurantifolii* C also down-regulates the *XTH* genes in *C. sinensis* (Cernadas *et al.*, 2008), suggesting that this repression plays a protective role in the defence response, limiting pathogen invasion. Furthermore, thickening of the cell wall by increased callose deposition is the first barrier, not only to *X. citri* infection in citrus plants (Enrique *et al.*, 2011), but also in other plant–bacterial interactions (Hauck *et al.*, 2003; Voigt, 2014; Yun *et al.*, 2006). In agreement with these results, the repression of *β-1,3-glucanase* and the reinforcement of the cell wall were observed in response to *X. citri* A^T, which are correlated with the beginning of cell death and the restriction of bacterial colonization in *C. limon*.

The repression of cellulose biosynthesis genes and the lignin biosynthetic pathways may lead to the accumulation of secondary metabolites. In Arabidopsis, cellulose synthase (*CESA7*)-deficient mutants showed increased resistance to a broad range of pathogens through the up-regulation of defence-related genes, including those involved in the accumulation of antimicrobial secondary metabolites (Hernandez-Blanco *et al.*, 2007). Moreover, Vanholme *et al.* (2012) proposed that a reduced flow of the lignin biosynthesis pathway may lead to a higher availability of substrates for the biosynthesis of phenolic compounds. In our work, GO analysis reveals that, although the category of 'lignin biosynthetic process' is not significantly represented, several categories related to phenylpropanoid pathways are enriched in the genes up-regulated by *X. citri* A^T. Accordingly, at early times post-inoculation, an increase in antimicrobial phenylpropanoids, including flavonoids and anthocyanins, is observed. Phenolic deposits have also been reported around the HR lesions triggered by *X. citri* in the 'Nagami' kumquat and calamondin resistant plants (Chen *et al.*, 2012).

Over recent years, significant progress has been made to understand the role of SA in the regulation of the plant defence response to pathogen attack (Fu and Dong, 2013; Kazan and Lyons, 2014). However, there are no data on the activation of SA-dependent defence in response to *X. citri* in citrus. Here, we show an accumulation of SA at early times of *X. citri* A^T inoculation, which is correlated with the beginning of HR-PCD in *C. limon*. Interestingly, at later stages of the defence response, although SA decreases to basal levels, the accumulation of phenolic compounds continues to increase. In Arabidopsis and maize, it has been proposed that flavones act as signalling molecules modulating the SA levels under abiotic and biotic stress conditions (Falcone *et al.*, 2015; Pourcel *et al.*, 2013). Our results show a temporal regulation of SA in the *X. citri* A^T resistance response, and suggest a coordinated regulation between SA and flavonoid pathways.

HR triggered by *X. citri* A^T involves autophagy-associated vacuolar processes protecting the plant from canker development

Autophagy has emerged as a central process in the regulation of pathogen-triggered HR. In recent years, several studies in model plants have shown that defence-related autophagy is involved in both cell survival (pro-survival; avoiding the spread of HR) and cell death (pro-death) (Hofius *et al.*, 2011; Lenz *et al.*, 2011; Seay and Dinesh-Kumar, 2005; Teh and Hofius, 2014; Zhou *et al.*, 2014). However, the mechanism governing this molecular switch is not well understood. In this work, we provide different lines of evidence indicating that *X. citri* A^T triggers an ETI-like response in *C. limon* which correlates with autophagic processes, which are temporally regulated. In recent years, it has been shown that SA signals play an important role in the induction of autophagy, which, in turn, operates as a negative regulator of SA-dependent signalling, restricting the spread of HR-PCD. In Arabidopsis, *ATG* mutants show an increase in SA levels leading to the ETI-associated spread of PCD during *P. syringae* effector AvrRPM1 challenge. These results suggest that autophagy is a critical mechanism for the control of HR-mediated PCD (Liu *et al.*, 2005; Xia *et al.*, 2013; Yoshimoto *et al.*, 2009). According to our results, the formation of autophagosome-like vesicles in survival cells and the reduction of the SA level at 7 dpi suggest that autophagy-associated vacuolar processes may also regulate the spread of cell death.

In Arabidopsis, the vacuole-mediated PCD triggered by the *P. syringae* effector AvrRPM1 is associated with two different

pathways: proteasome-regulated membrane fusion and the activation of vacuolar processing enzyme (VPE)-dependent defences (Hatsugai *et al.*, 2009; Rojo *et al.*, 2004). In this regard, we observed that vacuole-mediated cell death in *X. citri* A^T-induced HR-PCD in *C. limon* coincides with the up-regulation of γ-*VPE* and *ATG8f* genes (Tables S3 and S6). The accumulation of transcripts of the *ATG8* gene family has been reported in pathogen-infected Arabidopsis plants, and they are widely used to monitor the temporal regulation and subcellular dynamics of autophagy processes (Hofius *et al.*, 2011; Kabbage *et al.*, 2013; Yoshimoto *et al.*, 2004). In addition, an increase in the conversion of ATG8 to ATG8-PE suggests an active autophagic mechanism triggered by *X. citri* A^T.

In conclusion, our results suggest that *X. citri* A^T-triggered HR is mediated by a vacuolar membrane collapse that releases the antimicrobial content into the cytoplasm, causing cell death. Although, in *X. citri* A^T, we were unable to detect the presence of the *xopAG* effector gene (data not shown), other bacterial effectors should be involved in triggering HR-PCD in *C. limon*.

To our knowledge, this is the first report of the molecular mechanisms involved in HR induction by *X. citri* variants in commercially important citrus species, setting our results as a novel study to exploit the plant immune system as a biotechnological approach for the management of the disease. Moreover, the fact that pre-inoculation with *X. citri* A^T confers resistance to pathogenic *X. citri* establishes the basis for the eventual biological control of citrus canker.

EXPERIMENTAL PROCEDURES

Plant material, bacterial strains and pathogenicity assays

One-year-old 'Eureka' lemon [*C. limon* (L.) Burm. f.] plants grafted onto Troyer citrange and 'Clemenules' mandarin (*C. clementina* Hort. ex Tan.) plants grafted onto *Poncirus trifoliata* were kept under controlled conditions in a growth chamber. New shoots of approximately 1 cm in length, with at least five leaves, were selected for pathogenicity assays after pruning the plants. All the leaves on a new shoot were considered to be of the same ontological age (Favaro *et al.*, 2014).

Xanthomonas citri ssp. *citri* strains were transformed by electroporation with plasmid pMP2444 expressing GFP (Rigano *et al.*, 2007). Bacterial suspensions [10^9 colony-forming units (cfu)/mL] were prepared in 10 mM $MgCl_2$ and inoculated by spraying or cotton swab onto 15-day-old leaves of the new shoots. A 10 mM $MgCl_2$ solution was used as mock inoculation. Inoculated plants were maintained for 30 days in a growth chamber as reported previously (Enrique *et al.*, 2011). Disease progression was phenotypically monitored using an MVX10 stereomicroscope and photographed under white and UV light (520 nm). The canker lesions were quantified per square centimetre using Image J software (v1.41; National Institutes of Health, Bethesda, MD, USA).

The images in Figs 1, 2, 4 and 5 are representative results from three independent biological replicates, each involving three different plants and three different leaves per plant.

Biofilm analysis

Bacterial adhesion and biofilm formation *in vitro* were performed as described previously (Rigano *et al.*, 2007).

Biofilm formation *in vivo* was examined using GFP-tagged *X. citri* strains and an inverted confocal laser scanning microscope as described previously (Favaro *et al.*, 2014). Simulated three-dimensional images and sections were generated by the software Nikon EZ-C1 3.9 Free Viewer (Nikon Instruments Inc., Melville, NY, USA).

Histochemical and TEM assays

Cell death was visualized in *C. limon* leaves after staining with lactophenol–trypan blue, as described previously (Koch and Slusarenko, 1990). Autofluorescence of phenolic compounds was observed by fluorescence microscopy (excitation at 450–490 nm, emission at 520 nm) (Chen *et al.*, 2012) using free-hand leaf sections (Lux *et al.*, 2005). Observations were performed with an Olympus BX50F4 microscope (Olympus Optical Ltd. Company, Shinjuku, Tokyo, Japan).

For TEM experiments, leaf pieces (2×3 mm^2) were fixed in 4% (v/v) glutaraldehyde in phosphate buffer (1.8 g/L NaH_2PO_4, 23.25 g/L $Na_2HPO_4.7H_2O$ and 5 g/L NaCl, pH 7.4) for 24 h at 4 °C, and processed according to standard protocols. Sections were examined with a transmission electron microscope (JEOL-100CXII, Tokyo, Japan) at an accelerating voltage of 80 kV, and digital images were recorded with a ES1000W CCD digital camera (Gatan Inc., Pleasanton, CA, USA). The number of autophagosomes per cell in *C. limon* leaves was quantified at 7 and 20 days post-inoculation with *X. citri* A^T. At least 30 TEM images for each time point were used, which were representative of three independent experiments.

RNA preparation

Total RNA from *C. limon* leaves (4 g) was ground in liquid nitrogen and homogenized in 15 mL extraction buffer [200 mM Tris-HCl, pH 8.5; 200 mM sucrose; 30 mM magnesium acetate; 60 mM KCl; 0.5% (w/v) polyvinylpyrrolidone; 0.5% (w/v) sodium deoxycolate; 1% (w/v) sodium dodecylsulfate (SDS); 1% (w/v) sodium-*n*-lauroylsarcosine; 10 mM ethylenediaminetetraacetic acid (EDTA); 2% (v/v) β-mercaptoethanol]. The extraction procedure was performed as described previously (Marano and Carrillo, 1992). RNA samples were purified over Qiagen RNeasy mini-columns (Hilden, Germany).

Microarray experiments

Five inoculated leaves were randomly harvested at 48 hpi from three different plants and considered as independent biological replicates. Three biological replicates were performed.

RNA samples were amplified using the Amino Allyl MessageAmp™ II aRNA amplification kit (Applied Biosystems, Carlsbad, CA, USA). Reverse transcription, cDNA purification, dye coupling and fluorescent cDNA purification were performed according to the manufacturer's instructions. A

citrus microarray developed by the Interdisciplinary Center for Biotechnology Research (ICBR) of the University of Florida and Agilent Technologies Inc. (Palo Alto, CA, USA) was used. This microarray contains 44 000 probes based on citrus expressed sequence tags (ESTs) from Rutaceae (Febres *et al.*, 2012). Microarray hybridization was performed according to the manufacturer's instructions (Agilent Gene Expression Hybridization Kit, Agilent Technologies Inc.). The slides were scanned with GenePix Pro 4000B and analysed with GenePix6.0 software (Axon Instruments, Sunnyvale, CA, USA). Those features with a background-subtracted intensity lower than two-fold of the local background intensity in the two channels were discarded. Raw data were normalized as described in Martinez-Godoy *et al.* (2008). Only features with valid data in the three replicates were considered for further analysis.

Microarray data analysis

The identification of differentially expressed genes was performed using a significance analysis of microarrays (SAM) test (Tusher *et al.*, 2001). A 5% FDR and two-fold expression cut-off were considered to determine the up- and down-regulated genes. Functional analysis was carried out using FatiGO (Babelomics 4.0; Medina *et al.*, 2010), considering as statistically significant those GO terms having an adjusted *P* value of $\leq$0.05. Microarray data were deposited in the Gene Expression Omnibus (GEO) database under the accession number GSE78013.

qRT-PCR

The qRT-PCRs were performed according to Enrique *et al.* (2011). Reactions were carried out with real-time PCR master mix (Biodynamics SRL, Buenos Aires, Argentina) and monitored in a Mastercycler® ep realplex system (Eppendorf, Hamburg, Germany). The primers used in the experiments are listed in Table S1 (Mafra *et al.*, 2012) (see Supporting Information). Transcript levels were normalized against histone H4 (Shiotani *et al.*, 2007) using the $\Delta\Delta Ct$ method (Livak and Schmittgen, 2001). Non-treated (NT) lemon leaves served as the reference sample.

Quantification of UV-absorbing compounds and SA

Spectrophotometric determination of phenolic compounds was performed according to Mazza *et al.* (2000). Ten leaf discs (approximately 100 mg of fresh tissue) per sample were detached from *C. limon* plants at 48 hpi with each *X. citri* strain. The samples were homogenized in extraction solvent [99% (v/v) methanol in HCl] and incubated for 48 h at −20 °C. For flavonoid compounds, the absorbance of the extracts was read at 305 nm (A_{305}). For anthocyanin determination, the samples were re-extracted with 0.6 mL of chloroform and 0.3 mL of distilled water, vortexed and centrifuged (2 min at 3000 ***g***). The upper aqueous phases were collected and the anthocyanins were quantified by measurement of the absorbance at 530 nm (A_{530}), as described in Falcone *et al.* (2010). Mock inoculation with 10 mM $MgCl_2$ of *C. limon* leaves served as the reference sample.

For SA quantification, leaf samples were obtained as described for microarray experiments. Free SA was extracted from freeze-dried leaves (200 mg) homogenized in 5 mL of ultrapure water. Five microlitres of 50 ng [$^2H_4$]-SA were added before extraction as an internal standard. Samples were vortexed and centrifuged (15 min at 5000 ***g***). The supernatant was recovered. The pH was adjusted to 2.8 with acetic acid, and partitioned twice with an equal amount of diethyl ether (Durgbanshi *et al.*, 2005). The samples were evaporated to dryness at 35 °C, dissolved in 1.5 mL of methanol, filtered and evaporated at 35 °C. The dried extracts were dissolved in 50 μL of methanol and samples (10 μL) were injected directly into a liquid chromatograph (LC) coupled with electrospray tandem mass spectrometry (MS/MS, Quattro Ultima, Micromass, Manchester, UK). The liquid chromatographic and mass spectrometric analyses were performed according to Castillo *et al.* (2013).

Immunoblot analysis

Citrus limon leaves (100 mg) were ground in liquid nitrogen and homogenized in 500 μL of sample loading buffer [60 mM Tris, 10% (v/v) glycerol, 180 mM β-mercaptoethanol, 0.003% (w/v) bromophenol blue and 2% (w/v) SDS, pH 6.8]. The samples were boiled for 10 min at 100 °C prior to loading to the gels. Total protein samples (40 μg) were separated by urea-sodium dodecylsulfate-polyacrylamide gel electrophoresis (SDS-PAGE) [12% (w/v) acrylamide, 6 M urea] and electrophoretically transferred onto pre-wetted polyvinylidene difluoride membranes (PVDF-Immun-Blot®, BioRad, Hercules, CA, USA). Immunoblotting was performed using a polyclonal antibody with reactivity against Arabidopsis ATG8 (1 : 2000 dilution) (Agrisera, Vännäs, Sweden; Álvarez *et al.*, 2012), and then visualized using a peroxidase-conjugated goat anti-rabbit immunoglobulin G (IgG) (1 : 10 000 dilution) and Pierce™ ECL Western Blotting Substrate (Thermo Scientific, Petaluma, CA, USA) according to the manufacturers. Quantification of free ATG8 and ATG8-PE bands was performed by ImageJ analysis (v1.41; National Institutes of Health) of the immunoblot normalized against the Rubisco protein transferred to the membrane, as detected by Ponceau staining.

ACKNOWLEDGEMENTS

This work was principally supported by the Agencia Nacional de Promoción Científica y Tecnológica (PICT-2011-1833) to M.R.M. and by a grant from the Florida Citrus Research and Development Foundation to F.G.G. and M.R.M. M.A.C., A.A.V., A.P.C., M.P.F. and M.R.M. are Career Investigators of the Consejo Nacional de Investigaciones Científicas y Tecnológicas (CONICET). The authors thank J. M. Dow and G. Gudesblat for critical review of the manuscript.

REFERENCES

Álvarez, C., García, I., Moreno, I., Pérez-Pérez, M.E., Crespo, J.L., Romero, L.C. and Gotor, C. (2012) Cysteine-generated sulfide in the cytosol negatively regulates autophagy and modulates the transcriptional profile in Arabidopsis. *Plant Cell*, **24**, 4621–4634.

Bethke, G., Grundman, R.E., Sreekanta, S., Truman, W., Katagiri, F. and Glazebrook, J. (2014) Arabidopsis pectin methylesterases contribute to immunity against *Pseudomonas syringae*. *Plant Physiol.* **164**, 1093–1107.

Bilgin, D.D., Zavala, J.A., Zhu, J., Clough, S.J., Ort, D.R. and De Lucia, E.H. (2010) Biotic stress globally downregulates photosynthesis genes. *Plant Cell Environ.* **33**, 1597–1613.

Castillo, P., Escalante, M., Gallardo, M., Alemano, S. and Abdala, G. (2013) Effects of bacterial single inoculation and co-inoculation on growth and phytohormone production of sunflower seedlings under water stress. *Acta Physiol. Plant.* **35**, 2299–2309.

Cernadas, R.A., Camillo, L.R. and Benedetti, C.E. (2008) Transcriptional analysis of the sweet orange interaction with the citrus canker pathogens *Xanthomonas axonopodis* pv. *citri* and *Xanthomonas axonopodis* pv. *aurantifolii*. *Mol. Plant Pathol.* **9**, 609–631.

Chen, P.S., Wang, L.Y., Chen, Y.J., Tzeng, K.C., Chang, S.C., Chung, K.R. and Lee, M.H. (2012) Understanding cellular defence in kumquat and calamondin to citrus canker caused by *Xanthomonas citri* subsp. *citri*. *Physiol. Mol. Plant Pathol.* **79**, 1–12.

Chi, Y.H., Paeng, S.K., Kim, M.J., Hwang, G.Y., Melencion, S.M.B., Oh, H.T. and Lee, S.Y. (2013) Redox-dependent functional switching of plant proteins accompanying with their structural changes. *Front. Plant Sci.* **4**, 277. doi: 10.3389/fpls.2013.00277.

Chiesa, M.A., Siciliano, M.F., Ornella, L., Roeschlin, R.A., Favaro, M.A., Delgado, N.P., Sendín, L.N., Orce, I.G., Ploper, L.D., Vojnov, A.A., Vacas, J.G., Filippone, M.P., Castagnaro, A.P. and Marano, M.R. (2013) Characterization of a variant of *Xanthomonas citri* subsp. *citri* that triggers a host-specific defense response. *Phytopathology*, **103**, 555–564.

Deng, Z.N., Xu, L., Li, D.Z., Long, G.Y., Liu, L.P., Fang, F. and Shu, G.P. (2010) Screening citrus genotypes for resistance to canker disease (*Xanthomonas axonopodis* pv. *citri*). *Plant Breeding*, **129**, 341–345.

van Doorn, W.G., Beers, E.P., Dangl, J.L., Franklin-Tong, V.E., Gallois, P., Hara-Nishimura, I., Jones, A.M., Kawai-Yamada, M., Lam, E., Mundy, J., Mur, L.A., Petersen, M., Smertenko, A., Taliansky, M., Van Breusegem, F., Wolpert, T., Woltering, E., Zhivotovsky, B. and Bozhkov, P.V. (2011) Morphological classification of plant cell deaths. *Cell Death Differ.* **18**, 1241–1246.

Duan, Y.P., Castaneda, A., Zhao, G., Erdos, G. and Gabriel, D.W. (1999) Expression of a single, host-specific, bacterial pathogenicity gene in plant cells elicits division, enlargement, and cell death. *Mol. Plant–Microbe Interact.* **12**, 556–560.

Durgbanshi, A., Arbona, V., Pozo, O., Miersch, O., Sancho, J.V. and Gomez-Cadenas, A. (2005) Simultaneous determination of multiple phytohormones in plant extracts by liquid chromatography-electrospray tandem mass spectrometry. *J. Agric. Food Chem.* **53**, 8437–8442.

Enrique, R., Siciliano, F., Favaro, M.A., Gerhardt, N., Roeschlin, R., Rigano, L., Sendín, L., Castagnaro, A., Vojnov, A. and Marano, M.R. (2011) Novel demonstration of RNAi in citrus reveals importance of citrus callose synthase in defence against *Xanthomonas citri* subsp. *citri*. *Plant Biotechnol. J.* **9**, 394–407.

Escalon, A., Javegny, S., Vernière, C., Noel, L.D., Vital, K., Poussier, S., Hajri, A., Boureau, T., Pruvost, O., Arlat, M. and Gagnevin, L. (2013) Variations in type III effector repertoires, pathological phenotypes and host range of *Xanthomonas citri* pv. *citri* pathotypes. *Mol. Plant Pathol.* **14**, 483–496.

Falcone, M.L.F., Rius, S., Emiliani, J., Pourcel, L., Feller, A.J., Morohashi, K., Casati, P. and Grotewold, E. (2010) Cloning and characterization of an UV-B-inducible maize flavonol synthase. *Plant J.* **62**, 77–91.

Falcone, M.L.F., Emiliani, J., Rodriguez, E.J., Campos-Bermudez, V.A., Grotewold, E. and Casati, P. (2015) The identification of maize and Arabidopsis type I flavone synthases links flavones with hormones and biotic interactions. *Plant Physiol.* **169**, 1090–1107.

Favaro, M.A., Micheloud, N.G., Roeschlin, R.A., Chiesa, M.A., Castagnaro, A.P., Vojnov, A.A., Gmitter, F.G. Jr., Gadea, J., Rista, L.M., Gariglio, N.F. and Marano, M.R. (2014) Surface barriers of mandarin 'Okitsu' leaves make a major contribution to canker disease resistance. *Phytopathology*, **104**, 970–976.

Febres, V.J., Khalaf, A., Gmitter, F.G. Jr. and Moore, G.A. (2012) Evaluating gene expression responses of citrus to two types of defense inducers using a newly developed citrus Agilent microarray. *Acta Hortic.* **929**, 59–64.

Fu, X.Z., Gong, X.Q., Zhang, Y.X., Wang, Y. and Liu, J.H. (2012) Different transcriptional response to *Xanthomonas citri* subsp. *citri* between kumquat and sweet orange with contrasting canker tolerance. *PLoS One*, **7**, e41790.

Fu, Z.Q. and Dong, X. (2013) Systemic acquired resistance: turning local infection into global defense. *Annu. Rev. Plant Biol.* **64**, 839–863.

Graham, J.H., Gottwald, T.R., Cubero, J. and Achor, D.S. (2004) *Xanthomonas axonopodis* pv. *citri*: factors affecting successful eradication of citrus canker. *Mol. Plant Pathol.* **1**, 1–15.

Hatsugai, N., Iwasaki, S., Tamura, K., Kondo, M., Fuji, K., Ogasawara, K., Nishimura, M. and Hara-Nishimura, I. (2009) A novel membrane fusion-mediated plant immunity against bacterial pathogens. *Genes Dev.* **23**, 2496–2506.

Hauck, P., Thilmony, R. and He, S.Y. (2003) A *Pseudomonas syringae* type III effector suppresses cell wall-based extracellular defense in susceptible Arabidopsis plants. *Proc. Natl. Acad. Sci. USA*, **100**, 8577–8582.

Hernandez-Blanco, C., Feng, D.X., Hu, J., Sanchez-Vallet, A., Deslandes, L., Llorente, F., Berrocal-Lobo, M., Keller, H., Barlet, X., Sanchez-Rodriguez, C., Anderson, L.K., Somerville, S., Marco, Y. and Molina, A. (2007) Impairment of cellulose synthases required for Arabidopsis secondary cell wall formation enhances disease resistance. *Plant Cell*, **19**, 890–903.

Hofius, D., Schultz-Larsen, T., Joensen, J., Tsitsigiannis, D.I., Petersen, N.H.T., Mattsson, O., Jørgensen, L.B., Jones, J.D.G., Mundy, J. and Petersen, M. (2009) Autophagic components contribute to hypersensitive cell death in Arabidopsis. *Cell*, **37**, 773–783.

Hofius, D., Munch, D., Bressendorff, S., Mundy, J. and Petersen, M. (2011) Role of autophagy in disease resistance and hypersensitive response-associated cell death. *Cell Death Differ.* **18**, 1257–1262.

Jones, J.D. and Dangl, J.L. (2006) The plant immune system. *Nature*, **444**, 323–329.

Kabbage, M., Williams, B. and Dickman, M.B. (2013) Cell death control: the interplay of apoptosis and autophagy in the pathogenicity of *Sclerotinia sclerotiorum*. *PLoS Pathog.* **9**, e1003287. doi:10.1371/journal.ppat.1003287.

Kadota, Y., Sklenar, J., Derbyshire, P., Stransfeld, L., Asai, S., Ntoukakis, V., Jones, J.D., Shirasu, K., Menke, F., Jones, A. and Zipfel, C. (2014) Direct regulation of the NADPH oxidase RBOHD by the PRR-associated kinase BIK1 during plant immunity. *Mol. Cell*, **54**, 43–55.

Karpinski, S., Szechynska-Hebda, M., Wituszynska, W. and Burdiak, P. (2013) Light acclimation, retrograde signalling, cell death and immune defences in plants. *Plant Cell Environ.* **36**, 736–744.

Kazan, K. and Lyons, R. (2014) Intervention of phytohormone pathways by pathogen effectors. *Plant Cell*, **26**, 2285–2309.

Khalaf, A.A., Gmitter, F.G. Jr., Conesa, A., Dopazo, J. and Moore, G.A. (2011) *Fortunella margarita* transcriptional reprogramming triggered by *Xanthomonas citri* subsp. *citri*. *BMC Plant Biol.* **159**. doi:10.1186/1471-2229-11-159

Koch, E. and Slusarenko, A. (1990) Arabidopsis is susceptible to infection by a downy mildew fungus. *Plant Cell*, **2**, 437–445.

Lee, I.J., Kim, K.W., Hyun, J.W., Lee, Y.H. and Park, E.W. (2009) Comparative ultrastructure of nonwounded Mexican lime and Yuzu leaves infected with the citrus canker bacterium *Xanthomonas citri* pv. *citri*. *Microsci. Res. Technol.* **72**, 507–516.

Lenz, H.D., Haller, E., Melzer, E., Kober, K., Wurster, K., Stahl, M., Bassham, D.C., Vierstra, R.D., Parker, J.E., Bautor, J., Molina, A., Escudero, V., Shindo, T., van der Hoorn, R.A.L., Gust, A.A. and Nürnberger, T. (2011) Autophagy differentially controls plant basal immunity to biotrophic and necrotrophic pathogens. *Plant J.* **66**, 818–830.

Liu, Y., Schiff, M., Czymmek, K., Talloczy, Z., Levine, B. and Dinesh-Kumar, S.P. (2005) Autophagy regulates programmed cell death during the plant innate immune response. *Cell*, **121**, 567–577.

Liu, Y., Ren, D., Pike, S., Pallardy, S., Gassmann, W. and Zhang, S. (2007) Chloroplast-generated reactive oxygen species are involved in hypersensitive response-like cell death mediated by a mitogen-activated protein kinase cascade. *Plant J.* **51**, 941–954.

Livak, K.J. and Schmittgen, T.D. (2001) Analysis of relative gene expression data using real-time quantitative PCR and the 2(–Delta Delta C(T)) method. *Methods*, **25**, 402–408.

Lux, A., Morita, S., Abe, J. and Ito, K. (2005) An improved method for clearing and staining free-hand sections and whole-mount samples. *Ann. Bot.* **96**, 989–996.

Macho, A.P. and Zipfel, C. (2015) Targeting of plant pattern recognition receptor-triggered immunity by bacterial type-III secretion system effectors. *Curr. Opin. Microbiol.* **23**, 14–22.

Mafra, V., Kubo, K.S., Alves-Ferreira, M., Ribeiro-Alves, M., Stuart, R.M., Boava, L.P., Rodrigues, C.M. and Machado, M.A. (2012) Reference genes for accurate transcript normalization in citrus genotypes under different experimental conditions. *PLoS One*, **7**, e31263.

Malamud, F., Homem, R.A., Conforte, V.P., Yaryura, P.M., Castagnaro, A.P., Marano, M.R., do Amaral, A.M. and Vojnov, A.A. (2013) Identification and characterization of biofilm formation-defective mutants of *Xanthomonas citri* subsp. *citri*. *Microbiology*, **157**, 819–829.

Mammarella, N.D., Cheng, Z., Fu, Z.Q., Daudi, A., Bolwell, G.P., Dong, X. and Ausubel, F.M. (2014) Apoplastic peroxidases are required for salicylic acid-mediated defense against *Pseudomonas syringae*. *Phytochemistry*, **112**, 110–121.

Marano, M.R. and Carrillo, N. (1992) Constitutive transcription and stable RNA accumulation in plastids during the conversion of chloroplasts to chromoplasts in ripening tomato fruits. *Plant Physiol.* **100**, 1103–1113.

Martinez-Godoy, M.A., Mauri, N., Juarez, J., Marques, M.C., Santiago, J., Forment, J. and Gadea, J. (2008) A genome-wide 20 K citrus microarray for gene expression analysis. *BMC Genomics*, **9**, 318. doi: 10.1186/1471-2164-9-318.

Mazza, C.A., Boccalandro, H.E., Giordano, C.V., Battista, D., Scopel, A.L. and Ballare, C.L. (2000) Functional significance and induction by solar radiation of ultraviolet-absorbing sunscreens in field-grown soybean crops. *Plant Physiol.* **122**, 117–126.

Medina, I., Carbonell, J., Pulido, L., Madeira, S.C., Goetz, S., Conesa, A., Tarraga, J., Pascual-Montano, A., Nogales-Cadenas, R., Santoyo, J., García, F., Marbà, M., Montaner, D. and Dopazo, J. (2010) Babelomics: an integrative platform for the analysis of transcriptomics, proteomics and genomic data with advanced functional profiling. *Nucleic Acids Res.* **38**, W210–213. doi: 10.1093/nar/gkq388.

Pourcel, L., Irani, N.G., Koo, A.J.K., Bohorquez-Restrepo, A., Howe, G.A. and Grotewold, E. (2013) A chemical complementation approach reveals genes and interactions of flavonoids with other pathways. *Plant J.* **74**, 383–397.

Rigano, L.A., Siciliano, F., Enrique, R., Sendín, L., Filippone, P., Torres, P.S., Qüesta, J., Dow, J.M., Castagnaro, A.P., Vojnov, A.A. and Marano, M.R. (2007) Biofilm formation, epiphytic fitness, and canker development in *Xanthomonas axonopodis* pv. *citri*. *Mol. Plant–Microbe Interact.* **20**, 1222–1230.

Rojo, E., Martin, R., Carter, C., Zouhar, J., Pan, S., Plotnikova, J., Jin, H., Paneque, M., Sanchez-Serrano, J.J., Baker, B., Ausubel, F.M. and Raikhel, N.V. (2004) VPEgamma exhibits a caspase-like activity that contributes to defense against pathogens. *Curr. Biol.* **14**, 1897–1906.

Rybak, M., Minsavage, G.V., Stall, R.E. and Jones, J.B. (2009) Identification of *Xanthomonas citri* ssp. *citri* host specificity genes in a heterologous expression host. *Mol. Plant Pathol.* **10**, 249–262.

Schaad, N.C., Postnikova, E., Lacy, G.H., Sechler, A., Agarkova, I., Stromberg, P.E., Stromberg, V.K. and Vidaver, A.K. (2006) Emended classification of xanthomonad pathogens on citrus. *Syst. Appl. Microbiol.* **29**, 690–695.

Schaad, N.W., Postnikova, E., Lacy, G.H., Sechler, A., Agarkova, I., Stromberg, P.E., Stromberg, V.K. and Vidaver, A.K. (2005) Reclassification of *Xanthomonas campestris* pv. *citri* (ex Hasse 1915) Dye 1978 forms A, B/C/D, and E as *X. smithii* ssp. *citri* (ex Hasse) sp. nov. nom. rev. comb. nov., *X. fuscans* ssp. *aurantifolii* (ex Gabriel 1989) sp. nov. nom. rev. comb. nov., and *X. alfalfae* ssp. *citrumelo* (ex Riker and Jones) Gabriel 1989 sp. nov. nom. rev. comb. nov.; *X. campestris* pv. *malvacearum* (ex Smith 1901) Dye 1978 as *X. smithii* ssp. *smithii* nov. comb. nov. nom. nov.; *X. campestris* pv. *alfalfae* (ex Riker and Jones, 1935) dye 1978 as *X. alfalfae* ssp. *alfalfae* (ex Riker et al., 1935) sp. nov. nom. rev.; and "var. fuscans" of *X. campestris* pv. *phaseoli* (ex Smith, 1987) Dye 1978 as *X. fuscans* ssp. *fuscans* sp. nov. *Syst. Appl. Microbiol.* **28**, 494–518.

Seay, M.D. and Dinesh-Kumar, S.P. (2005) Life after death: are autophagy genes involved in cell death and survival during plant innate immune responses? *Autophagy*, **1**, 185–186.

Shapiguzov, A., Vainonen, J.P., Wrzaczek, M. and Kangasjarvi, J. (2012) ROS-talk-how the apoplast, the chloroplast, and the nucleus get the message through. *Front. Plant Sci.* **3**, 292. doi: 10.3389/fpls.2012.00292.

Shiotani, H., Fujikawa, T., Ishihara, H., Tsuyumu, S. and Ozaki, K. (2007) A *pthA* homolog from *Xanthomonas axonopodis* pv. *citri* responsible for host-specific suppression of virulence. *J. Bacteriol.* **189**, 3271–3279.

Soprano, A.S., Abe, V.Y., Smetana, J.H. and Benedetti, C.E. (2013) Citrus MAF1, a repressor of RNA polymerase III, binds the *Xanthomonas citri* canker elicitor PthA4 and suppresses citrus canker development. *Plant Physiol.* **163**, 232–242.

Sun, X., Stall, R.E., Jones, J.B., Cubero, J., Gottwald, T.R., Graham, J.H., Dixon, W.N., Schubert, T.S., Chaloux, P.H. and Stromberg, V.K. (2004) Detection and characterization of a new strain of citrus canker bacteria from Key/Mexican lime and alemow in South Florida. *Plant Dis.* **88**, 1179–1188.

Supek, F., Bošnjakn, M., Škunca, N. and Šmuc, T. (2011) REVIGO summarizes and visualizes long lists of Gene Ontology terms. *PLoS One*, **6**, e21800.

Teh, O.K. and Hofius, D. (2014) Membrane trafficking and autophagy in pathogen-triggered cell death and immunity. *J. Exp. Bot.* **65**, 1297–1312.

Tusher, V.G., Tibshirani, R. and Chu, G. (2001) Significance analysis of microarrays applied to the ionizing radiation response. *Proc. Natl. Acad. Sci. USA*, **98**, 5116–5121.

Vanholme, R., Storme, V., Vanholme, B., Sundin, L., Christensen, J.H., Goeminne, G., Halpin, C., Rohde, A., Morreel, K. and Boerjan, W. (2012) A systems biology view of responses to lignin biosynthesis perturbations in Arabidopsis. *Plant Cell*, **24**, 3506–3529.

Vernière, C., Hartung, J.S., Pruvost, O.P., Civerolo, E.L., Alvarez, A.M., Maestri, P. and Luisetti, J. (1998) Characterization of phenotypically distinct strains of *Xanthomonas axonopodis* pv. *citri* from Southwest Asia. *Eur. J. Plant Pathol.* **104**, 477–487.

Voigt, C.A. (2014) Callose-mediated resistance to pathogenic intruders in plant defense-related papillae. *Front. Plant Sci.* **5**, 168. doi: 10.3389/fpls.2014.00168.

Vojnov, A. and Marano, M.R. (2015) Biofilm formation and virulence in bacterial plant pathogens. In: *Virulence Mechanisms of Plant-Pathogenic Bacteria* (Wang, N., Jones, J.B., Sundin, G.W., White, F.F., Hogenhout, S.A., Roper, C., De la Fuente, L. and Ham, J.H., eds), pp. 21–34. St. Paul, Minnesota: The American Phytopathological Society APS Press.

Vojnov, A.A., do Amaral, A.M., Dow, J.M., Castagnaro, A.P. and Marano, M.R. (2010) Bacteria causing important diseases of citrus utilise distinct modes of pathogenesis to attack a common host. *Appl. Microbiol. Biotechnol.* **87**, 467–477.

Wrzaczek, M., Brosché, M. and Kangasjärvi, J. (2013) ROS signaling loops—production, perception, regulation. *Curr. Opin. Plant Biol.* **16**, 575–582.

Xia, P., Wang, S., Du, Y., Xhao, Z., Shi, L., Sun, L., Huang, G., Ye, B., Li, C., Dai, Z., Hou, N., Cheng, X., Sun, Q., Li, L., Yang, X. and Fan, Z. (2013) WASH inhibits autophagy through suppression of Beclin 1 ubiquitination. *EMBO J.* **32**, 2685–2696.

Yoshimoto, K., Hanaoka, H., Sato, S., Kato, T., Tabata, S., Noda, T. and Ohsumia, Y. (2004) Processing of ATG8s, ubiquitin-like proteins, and their deconjugation by ATG4s are essential for plant autophagy. *Plant Cell*, **16**, 2967–2983.

Yoshimoto, K., Jikumaru, Y., Kamiya, Y., Kusano, M., Consonni, C., Panstruga, R., Ohsumi, Y. and Shirasu, K. (2009) Autophagy negatively regulates cell death by controlling NPR1-dependent salicylic acid signaling during senescence and the innate immune response in Arabidopsis. *Plant Cell*, **21**, 2914–2927.

Yun, M.H., Torres, P.S., El Oirdi, M., Rigano, L.A., Gonzalez-Lamothe, R., Marano, M.R., Castagnaro, A.P., Dankert, M.A., Bouarab, K. and Vojnov, A.A. (2006) Xanthan induces plant susceptibility by suppressing callose deposition. *Plant Physiol.* **141**, 178–187.

Zhou, J., Yu, J.Q. and Chen, Z. (2014) The perplexing role of autophagy in plant innate immune responses. *Mol. Plant Pathol.* **15**, 637–645.

SUPPORTING INFORMATION

Additional Supporting Information may be found in the online version of this article at the publisher's website:

Fig. S1 Bacterial adhesion and biofilm formation on an inert plastic surface.

Fig. S2 Venn diagrams representing the distribution of regulated transcripts in *Citrus limon* after *Xanthomonas citri* ssp. *citri* (*X. citri*) inoculation.

Fig. S3 Phenolic compound accumulation surrounding the hypersensitive response associated with rapid programmed cell death (HR-PCD) induced by *Xanthomonas citri* ssp. *citri* A^T.

Fig. S4 Transmission electron microscopy of *Citrus clementina* leaves inoculated with *Xanthomonas citri* ssp. *citri* (*X. citri*) strains.

Table S1 List of all oligonucleotide primers used for quantitative reverse transcription-polymerase chain reaction (qRT-PCR) analysis.

Table S2 Microarray expression data for up- and down-regulated genes in response to *Xanthomonas citri* ssp. *citri (X. citri)* strains in *Citrus limon* leaves.

Table S3 Comparison of microarray expression data for up- and down-regulated genes in *Citrus limon* leaves in response to *Xanthomonas citri* ssp. *citri (X. citri)* strains.

Table S4 Gene ontology (GO) 'biological process' terms enriched in the differentially expressed genes unique to the *Citrus limon–Xanthomonas citri* ssp. *citri* strain A^T interaction.

Table S5 Gene ontology (GO) 'biological process' terms enriched in the differentially expressed genes unique to the *Citrus limon–Xanthomonas citri* ssp. *citri* strain T interaction.

Table S6 Quantitative reverse transcription-polymerase chain reaction (qRT-PCR) analysis of genes involved in the defence and pathogenesis response to *Xanthomonas citri* ssp. *citri* (*X. citri*) strains.